UDC 551.465

S. Patil, V.P. Singh

Effect of vertically logarithmic steady current on shallow surface waves

The combine wave-current flow has been solved by researchers by assuming wave over either depth-wise constant or linearly current profile. Some complicated non-linear current profiles have also been considered to simulate various shear currents. In this paper, a non-linear current, vertically logarithmic in nature is considered and its interaction with a periodic surface wave is examined. Navier-Stokes equations for incompressible flow are solved for the current part and by using periodic boundary conditions; effect of logarithmic current on wave components is assessed. The corresponding celerity and dispersion equation yields a close form solution for the shallow wave approximation. Several comparative trends between wave-only, wave with log current and with constant current for the wave following/opposing these currents have been discussed. The flow properties of the first order are presented which can be applicable to the real inland and coastal flows where progressive waves are ubiquitous over depth-wise logarithmic current. The work is further extended to the second order semi-empirical wave component using past experimental data on wave spectrum of combine flow.

1. Introduction. Several working groups like atmospheric sciences, oceanography, including waves, and remote sensing have investigated the benefits of coastal and estuarine hydrodynamics where the topic of combine wave-current flow is of immense importance. When a surface wave meets a steady current underneath, it undergoes change in amplitude during adaptation process [1] to reach to a steady state after which the combine profile remains permanent over space and time. The interaction shows that waves are strained and refracted by currents and exchange of impulse, momentum, and energy occurs between the waves and mean flow. This causes change in the magnitude of current at the bottom and surface [2] and also change in the flow properties such as horizontal and vertical velocities, turbulent characteristics, pressure and energy distributions, etc [3]. Mixing due to waves and currents greatly enhances the transfer of chemical and biological elements, especially in the coastal zone. Wave induced orbital velocity causes erosion of sediments which are advected by the steady current [4]. The wave flumes or the offshore basins in hydrodynamic laboratory are therefore, designed especially to provide precise scaled-versions of various wave-current combinations. In the experiments on wave-current is used a sheared current having vertical profile almost linear near the free surface but very much curved near the bottom [5 – 7]. This current profile can be simulated by well-known logarithmic law [3]. Examples of combine wave over depth-wise logarithmic current flow (hereto denoted as wave-log current, see Fig. 1) are: uniform flow in open channel with surface waves due to ubiquity of wind shear or long-period tides in costal zones. The vertical current profile in these flows is nearly logarithmic. Accurate modeling of this flow pattern is important for dispersion and diffusion studies, geophysical understanding and coastal construction because any approximation to the existing wave-log current may lead to numerous biases in the results. This note presents the formulation and properties of the wave-log current flow. A brief literature review on wave-current interaction is as follows.

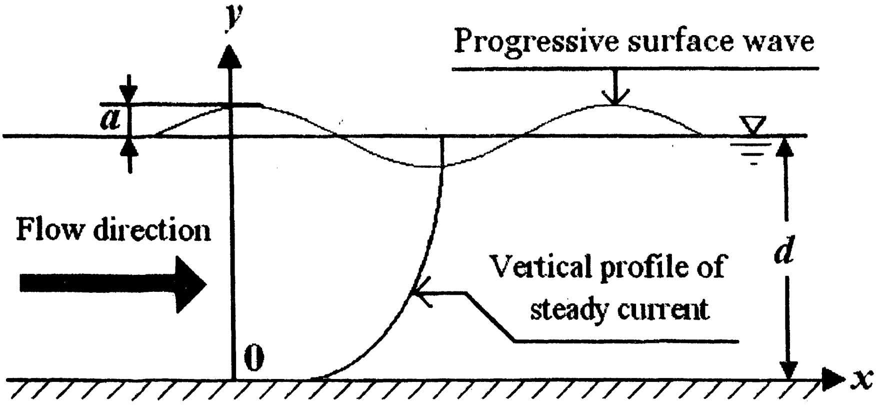

Fig. 1. Combine wave-log current flow field

2. Literature review. Past studies on wave-current interaction have approximated current component as depth-wise -constant, -linear or -nonlinear. The simplest form is the depth-wise constant current under sinusoidal wave [8, 9] which is extended for non-linear waves in [10] using velocity potential and in [11] using stream function. Wave diffraction over a shoal- and wave-constant current interaction was studied in [12].

In case of depth-dependent current, it is assumed in paper [13] depth-wise linear current under wave to study surface displacement and particle velocities. In [14] was used stream function approach [11] to simulate non-linear waves on linear current and has been numerically studied in [15] and also in [16] using vorticity in terms of shear current. Models that predict the steady-state of the interaction, using given wave pattern and linear current, were proposed in [17, 18]. However, due to the linear nature of current, these models fail to simulate the non-linear current in the real flows in field especially when real flows are measured by high-resolution instruments like Synthetic Aperture Radars, ENVISAT, SWIMSAT, etc. Indeed, it is necessary for maritime structures like ship, floating and fixed platform to be accurately tested for there performances in the real hydrodynamic environment.

The depth-wise nonlinear current under wave has been modeled by using a cluster of straight lines [19]. Waves with bilinear current profiles in deep water are studied in [20] and in [21] for shallow water. A more complicated current profile was considered in [22] by dividing the fluid in two regions of differing vorticity which had been further modified in [23] by using $1/7^{th}$ law to present combine stream function and dispersion relation. Authors of [24] used mixing length hypothesis to derive mathematical model for mean velocity under waves in current direction. Some solutions in terms of hypergeometric function for the waves with various shearing profiles are included in [25]. A power series velocity equation derived in [26] based on Prandtl momentum-transfer theory but requires an exponent to be determined empirically for current-only as well as wave-current case [3]. The slow deformation of propagating waves over a given slowly-varying uniform current were described in [18, 27]; however such current profile is difficult to be known a priory. Author of [28] induced the non-linearity in the current profile by WKB approximation (weakly nonlinear); by multiplying linear profile with a parameter and also by providing it a wave-induced shift. The current profiles were complex functions and provided good agreement with experiments. The dispersion relation for waves on depth-wise exponential shear current was examined in [29 – 31] and further studied in [32] using stream function theory to consider wave characteristics. The dispersion relations for these cases, which assign the appropriate wave number to the given wave period, has also been determined in [23] using a WKB approach and more generally in [33, 34]. These assumed current profiles were in the form of trigonometric and hyperbolic functions and hence complex.

In this note, depth-wise log-current is used as a nonlinear case of shear current and its effect on the surface periodic wave is investigated. In addition to the mean flow velocity, the rotational nature of the shear current changes the wave characteristics [35]. The resultant model is in the form of a combine stream function $\psi(x, y, t)$ for two-dimensional, incompressible steady flow with a surface periodic wave where x, y are the flow and vertical directions, respectively and t is the time. Thus, the log-current for the turbulent flow $u_l = (u_* / k_v)\ln(30y/k_s)$ in simplified form can be written as

$$u_l = \frac{u_*}{k_v}\ln\frac{y}{k_s} + U_c, \tag{1}$$

where $U_c = 3.7u_*$ [36], u_* is the shear velocity, k_v = 0.4 is the von Karman's constant, and k_s is the Nikurandze's roughness coefficient. It was shown in [37, pp. 16, 17] that (1) is valid near bottom region and for far region, equation (1) with a wake function [38] should be used. However, in practical applications, equation (1) is still commonly assumed to describe the velocity distribution over the entire depth of uniform, steady open-channel flows. The shear in (1) provides vorticity and with a surface wave, forms two-dimensional rotational periodic flow. In absence of shear (constant-velocity case), u_* = 0 and $U_c = \overline{U}$ (mean flow velocity) is substituted in (1) which provides $u_l = \overline{U}$ and the flow becomes two-dimensional irrotational periodic flow. To derive the combine stream function, the stream function of (1) (current part), i.e.

$$\psi_1 = \int u_l\,dy = \frac{u_*}{k_v}\left(y\ln\frac{y}{k_s} - y\right) + U_c\,y + B_3$$

is taken a priory (B_3 is a constant and is zero for the horizontal bottom) and the stream function for the wave components influenced by the current part are derived using wave theory. The approach is inverse to that given by authors of [17], who assumed wave component a priory and derived current component which however, is depth-wise linear current profile. The celerity, dispersion relation and the flow properties for wave-log current to the first order of wave amplitude are presented. The second order wave is also empirically simulated by using experimental data (see, [3]).

3. Formulation of wave-log current flow. The equations of motion neglecting the viscous effect can be written as

$$\rho\left(\frac{\partial u}{\partial t}+u\frac{\partial u}{\partial x}+v\frac{\partial u}{\partial y}\right)=-\frac{\partial p}{\partial x}, \tag{2a}$$

$$\rho\left(\frac{\partial v}{\partial t}+u\frac{\partial v}{\partial x}+v\frac{\partial v}{\partial y}\right)=-\frac{\partial p}{\partial y}-\rho g, \tag{2b}$$

where ρ is the constant density, p is the pressure in the fluid, g is the acceleration due to gravity, t is the time, x is the flow direction and y is the vertical direction measured from the channel bottom. Also $u=\partial\psi/\partial y$ and $v=-\partial\psi/\partial x$ are the velocity components in x and y direction respectively where ψ is the stream function. Equations (2a) and (2b) are integrated over x and y respectively. Using continuity equation $\partial u/\partial x+\partial v/\partial y=0$ and conservation of vorticity and eliminating pressure terms, the resultant two-dimensional equation of motion for an incompressible, inviscid fluid is written as [17]

$$\left(\frac{\partial}{\partial t}+\vec{V}\cdot\nabla\right)\nabla^2\psi=0, \tag{3}$$

where $\nabla=\frac{\partial}{\partial x}\vec{i}+\frac{\partial}{\partial y}\vec{j}$ is the two-dimensional gradient operator, $\nabla^2=\frac{\partial^2}{\partial x^2}+\frac{\partial^2}{\partial y^2}$ is the two-dimensional Laplacian operator and $\vec{V}=\frac{\partial\psi}{\partial y}\vec{i}-\frac{\partial\psi}{\partial x}\vec{j}$ is the velocity vector. Substituting these quantities in equation (3), it becomes

$$\left[\frac{\partial^3\psi}{\partial t\partial x^2}+\frac{\partial^3\psi}{\partial t\partial y^2}\right]+\frac{\partial\psi}{\partial y}\left[\frac{\partial^3\psi}{\partial x^3}+\frac{\partial^3\psi}{\partial x\partial y^2}\right]-\frac{\partial\psi}{\partial x}\left[\frac{\partial^3\psi}{\partial y\partial x^2}+\frac{\partial^3\psi}{\partial y^3}\right]=0. \tag{3a}$$

The velocity perpendicular to the flat bottom at $y=0$ is zero. This provides horizontal bottom condition as

$$-\frac{\partial\psi}{\partial x}=0 \quad \text{at } y=0. \tag{4}$$

Further, the free surface kinematic boundary condition can be written as

$$\left(\frac{\partial}{\partial t}+\vec{V}\cdot\nabla\right)S=0 \quad \text{on } y=\eta\,(x,t), \tag{5}$$

where η is the wave surface. The dynamic free surface boundary condition is given as

$$-g\eta+\int\left(\frac{\partial^2}{\partial t\partial x}+\vec{V}\cdot\frac{\partial}{\partial x}\nabla\right)\psi dy=F_2(x,t) \quad \text{on } y=\eta(x,t) \tag{6}$$

for some function $F_2(x, t)$. Moreover, the free surface condition can be written as

$$S(x,y,t)= y-\eta(x,t)=0. \qquad (7)$$

Neglecting the viscous dissipation at sidewalls, the wave is assumed to be periodic and permanent type. Therefore the free surface can be represented by Fourier series in $(kx - \sigma t)$ as

$$\eta(x,t)=\sum_{n=0}^{\infty} a_n \cos n(kx-\sigma t), \qquad (8)$$

where a_n are the Fourier coefficients, $k = 2\pi / L$ is the wave number, $\sigma = 2\pi / T$ is the wave frequency, L is the wavelength, T is the wave period and n is the order of equation (8). In view of (8), ψ must also be a periodic function as $\psi(x,y,t) = \psi(kx-\sigma t, y)$ and therefore for the horizontal bed, can be written as

$$\psi(x,y,t)=\sum_{n=0}^{\infty} A_n(y)\cos n(kx-\sigma t), \qquad (9)$$

where $A_n(y)$ are the coefficients depend on the order n in the Taylor's expansion and are determined in the next section. According to the proper choice of the $A_n(y)$, the stream function can be described for wave-only case, current-only case or combined wave-log current case. Taylor's expansion of (8) and (9) to the first order can be written as

$$\eta(x,t)=d+ a\cos(kx-\sigma t), \qquad (10)$$

$$\psi(x,y,t)=A_0(y)+ A_1(y)\cos(kx-\sigma t), \qquad (11)$$

where $a_1 = a$ is the wave amplitude in equation (10) and d is the flow depth. The stream function $A_0(y)$ in (11) corresponds to the log-current velocity given by equation (1). The corresponding stream function $A_0(y)$ is now known a priory and can be given as

$$A_0(y)=\int\left(U_c+\frac{u_*}{k_v}\ln\frac{y}{k_s}\right)dy= U_c y+\frac{u_*}{k_v}\left(y\ln\frac{y}{k_s}-y\right)+B_3. \qquad (12)$$

Now, equation (3) is used to find expressions for A_1 in (11) to the first order of wave amplitude. Thus substituting equation (12) in (3), equation (3) becomes

$$\begin{bmatrix} \sigma A_1''-\sigma k^2 A_1+U_c k^3 A_1+\left(\frac{u_*}{k_v}k^3\ln\frac{y}{k_s}\right)A_1- \\ -U_c k A_1''-\left(\frac{u_*}{k_v}k\ln\frac{y}{k_s}\right)A_1''-\frac{u_* k}{k_v y^2}A_1 \end{bmatrix}\sin(kx-\sigma t)+ \qquad (13)$$

$$+\frac{1}{2}(-k A_1' A_1''+k A_1 A''')\sin 2(kx-\sigma t)=0,$$

where the prime denotes differentiation with respect to y. Equation (13) suggests that for all $(kx - \sigma t)$, a set of differential equations are

$$\sigma A_1'' - \sigma k^2 A_1 + U_c k^3 A_1 + \left(\frac{u_*}{k_v} k^3 \ln\frac{y}{k_s}\right) A_1 - U_c k A_1'' - \left(\frac{u_*}{k_v} k \ln\frac{y}{k_s}\right) A_1'' - \frac{u_* k}{k_v y^2} A_1 = 0, \quad (14)$$

$$-k A_1' A_1'' + k A_1 A_1''' = 0. \quad (15)$$

Equation (15) is the differential equation for wave-only flow. From (4), $\psi = 0$ for $y = 0$. For this, the periodic part of (11) suggests $A_1(y) = 0$ at $y = 0$ and (15) suggests

$$A_1(y) = B_4 \operatorname{sh}(my), \quad (16)$$

where B_4 is a constant to be determined. Substitution of equation (16) for $m = k$ in (14), equation (14) reduces to $-\frac{u_* k}{k_v y^2} B_4 \operatorname{sh}(ky) = 0$. This expression satisfies for the condition of $\operatorname{sh}(kd) \to 0$ (replaced $y = d$), which is true for shallow water waves ($d/L < 0.05$; $kd < 0.314$) dealt with in this paper. Thus equation (14) satisfies (1) and therefore validates a priory assumed log-current profile. For $m > k$ and $m < k$, trigonometric current profiles result [17] and is out of scope of present topic. Substituting A_0 (see, equation (12)) and A_1 from (16) with $m = k$ in equation (11), the stream function for the wave-log current flow is

$$\psi(x, y, t) = \frac{u_*}{k_v}\left(y \ln\frac{y}{k_s} - y\right) + U_c y + B_3 + B_4 \operatorname{sh}(ky) \cos(kx - \sigma t), \quad (17)$$

where the constant $B_3 = 0$ as for the flat bottom $y = 0$, and thus it is must that $\psi(x, y, t) = 0$ for all t.

The coefficient B_4 in (17) now can be determined by applying kinematic free surface boundary condition (equation (5)). Substituting $\nabla = \frac{\partial}{\partial x}\vec{i} + \frac{\partial}{\partial y}\vec{j}$, $\vec{V} = \frac{\partial \psi}{\partial y}\vec{i} - \frac{\partial \psi}{\partial x}\vec{j}$ and (7), equation (5) simplified as

$$\frac{\partial y}{\partial t} - \frac{\partial \eta}{\partial t} + \left(\frac{\partial \psi}{\partial y}\vec{i} - \frac{\partial \psi}{\partial x}\vec{j}\right)\left(\frac{\partial}{\partial x}\vec{i} + \frac{\partial}{\partial y}\vec{j}\right)(y - \eta) = 0,$$

$$\frac{\partial y}{\partial t} - \frac{\partial \eta}{\partial t} + \left(\frac{\partial \psi}{\partial y}\frac{\partial}{\partial x} - \frac{\partial \psi}{\partial x}\frac{\partial}{\partial y}\right)(y - \eta) = 0,$$

$$\frac{\partial y}{\partial t} - \frac{\partial \eta}{\partial t} + \left(\frac{\partial \psi}{\partial y}\frac{\partial y}{\partial x} - \frac{\partial \psi}{\partial x}\frac{\partial y}{\partial y}\right) - \left(\frac{\partial \psi}{\partial y}\frac{\partial \eta}{\partial x} - \frac{\partial \psi}{\partial x}\frac{\partial \eta}{\partial y}\right) = 0.$$

As $\partial y / \partial t = 0$, $\partial y / \partial x = 0$, $\partial \eta / \partial y = 0$, the equation becomes

$$\frac{\partial\eta}{\partial t}+\frac{\partial\psi}{\partial y}\frac{\partial\eta}{\partial x}+\frac{\partial\psi}{\partial x}=0. \tag{18}$$

Equation (18) is the simplified kinematic free surface boundary condition to the first order and is to be satisfied at $y = d$. Substituting (10) and (17) in (18), equation (18) becomes

$$a\sigma\sin(kx-\sigma t)-\frac{u_*}{k_v}ak\ln\frac{y}{k_s}\sin(kx-\sigma t)-U_c ak\sin(kx-\sigma t)-$$

$$-\frac{ak^2}{2}B_4\sin 2(kx-\sigma t)\mathrm{ch}(ky)-B_4k\mathrm{sh}(ky)\sin(kx-\sigma t)=0.$$

The term consisting $\sin 2(kx-\sigma t)$ corresponds to second order expansion and hence neglected. From the remaining terms and $y = d$, B_4 can be given as

$$B_4=\frac{a}{\mathrm{sh}(kd)}\left[C-\frac{u_*}{k_v}\ln\frac{d}{k_s}-U_c\right]. \tag{19}$$

Substituting (19) in (17), the corresponding stream function to the first order is

$$\psi(x,y,t)=\frac{u_*}{k_v}\left(y\ln\frac{y}{k_s}-y\right)+U_c y+a\left(C-\frac{u_*}{k_v}\ln\frac{d}{k_s}-U_c\right)\frac{\mathrm{sh}(ky)}{\mathrm{sh}(kd)}\cos(kx-\sigma t), \tag{20}$$

where $C = \sigma/k$ is the absolute celerity. The influence of log-current in the fluid domain can be judged from equation (20). Several flow characteristics in the combine flow domain of wave-log current can be studied from (20) too. Some of them are included in section 5. Equation (20) can be modified for wave-constant current case by substituting $u_* = 0$ and $U_c=\overline{U}$ in (20).

4. Celerity and dispersion relation for wave-log current (first-order approximation). The dynamic free surface boundary condition of constant pressure on the free surface is used to determine the dispersion equation. Equation (6) to the first order can be written as

$$-g\frac{\partial\eta}{\partial x}+\frac{\partial}{\partial x}\int\left[\frac{\partial^2}{\partial t\,\partial x}+\vec{V}\cdot\frac{\partial}{\partial x}\nabla\right]\psi\,dy=0. \tag{21}$$

Substituting $\vec{V}=\frac{\partial\psi}{\partial y}\vec{i}-\frac{\partial\psi}{\partial x}\vec{j}$ and $\nabla=\frac{\partial}{\partial x}\vec{i}+\frac{\partial}{\partial y}\vec{j}$ in equation (21),

$$-g\frac{\partial\eta}{\partial x}+\frac{\partial}{\partial x}\int\left[\frac{\partial^2}{\partial t\,\partial x}+\left(\frac{\partial\psi}{\partial y}\vec{i}-\frac{\partial\psi}{\partial x}\vec{j}\right)\cdot\left(\frac{\partial^2}{\partial x^2}\vec{i}+\frac{\partial^2}{\partial x dy}\vec{j}\right)\right]\psi\,dy=0.$$

Note that, ψ for the second term of bracketed part will place in the empty place of second derivative. The simplified form of equation (21) is

$$-g\frac{\partial\eta}{\partial x}+\frac{\partial}{\partial x}\int\frac{\partial^2\psi}{\partial t\,\partial x}dy+\frac{\partial}{\partial x}\int\left(\frac{\partial\psi}{\partial y}\frac{\partial^2\psi}{\partial x^2}-\frac{\partial\psi}{\partial x}\frac{\partial^2\psi}{\partial x dy}\right)dy=0 \qquad (21a)$$

and is to be satisfied on $y = d$. Substituting equations (10) and (20) in equation (21a), the three terms of equation (21a) are as follows. The first, second and third terms are

$$-g\frac{\partial\eta}{\partial x}=g\,a\,k\sin(kx-\sigma t),$$

$$\frac{\partial}{\partial x}\int\frac{\partial^2\psi}{\partial t\,\partial x}dy=-k\sigma\,a\left(C-\frac{u_*}{k_v}\ln\frac{d}{k_s}-U_c\right)\frac{\mathrm{ch}(ky)}{\mathrm{sh}(kd)}\cos(kx-\sigma t),$$

$$\int\left(\frac{\partial\psi}{\partial y}\frac{\partial^2\psi}{\partial x^2}-\frac{\partial\psi}{\partial x}\frac{\partial^2\psi}{\partial y^2}\right)dy=-\frac{k^2a}{\mathrm{sh}(kd)}\left(C-\frac{u_*}{k_v}\ln\frac{d}{k_s}-U_c\right)\left(\frac{u_*}{k_v}\right)\Im\cos(kx-\sigma t)-$$

$$-k^2a^2\left(C-\frac{u_*}{k_v}\ln\frac{d}{k_s}-U_c\right)^2\frac{\mathrm{ch}(2ky)}{4\mathrm{sh}(kd)}-ka\overline{U}\left(C-\frac{u_*}{k_v}\ln\frac{d}{k_s}-U_c\right)\frac{\mathrm{ch}(ky)}{\mathrm{sh}(kd)}\cos(kx-\sigma t).$$

The calculation involves integral $\Im=\int\ln(y/k_s)\mathrm{sh}(ky)dy$. Following approximation for shallow water waves, i. e., $d/L\le 0.05$, close form solution of the integral is derived as

$$\Im=\int\ln\frac{y}{k_s}\mathrm{sh}(ky)dy=\frac{1}{k}\ln\frac{y}{k_s}\mathrm{ch}(ky)-\frac{1}{k}\left[\ln\frac{y}{k_s}+\frac{(ky)^2}{4}\right].$$

The derivation is included in Appendix (see, equation (A6)). Another solution by way of $Ei(z)$ function (exponential integral function) is also presented in the Appendix. Finally the x derivative of the third term is

$$\frac{\partial}{\partial x}\int\left(\frac{\partial\psi}{\partial y}\frac{\partial^2\psi}{\partial x^2}-\frac{\partial\psi}{\partial x}\frac{\partial^2\psi}{\partial x dy}\right)dy=\frac{k^3a}{\mathrm{sh}(kd)}\left[C-\frac{u_*}{k_v}\ln\frac{d}{k_s}-U_c\right]\left(\frac{u_*}{k_v}\right)\Im\sin(kx-\sigma t)+$$

$$+k^2a\overline{U}\left[C-\frac{u_*}{k_v}\ln\frac{d}{k_s}-U_c\right]\frac{\mathrm{ch}(ky)}{\mathrm{sh}(kd)}\sin(kx-\sigma t).$$

Substituting the solution of $\Im$, the third term is rewritten as

$$k^2a\left[C-\frac{u_*}{k_v}\ln\frac{d}{k_s}-U_c\right]\left(\frac{u_*}{k_v}\right)\ln\frac{y}{k_s}\cdot\frac{\mathrm{ch}(ky)}{\mathrm{sh}(kd)}\sin(kx-\sigma t)-$$

$$-\frac{k^2a\left[C-\frac{u_*}{k_v}\ln\frac{d}{k_s}-U_c\right]\left(\frac{u_*}{k_v}\right)T_1}{\mathrm{sh}(kd)}\sin(kx-\sigma t)+$$

$$+k^2 a\bar{U}\left[C-\frac{u_*}{k_v}\ln\frac{d}{k_s}-U_c\right]\frac{\mathrm{ch}(ky)}{\mathrm{sh}(kd)}\sin(kx-\sigma t),$$

where $T_1=\ln(y/k_s)+(ky)^2/4$. Alternatively $T_1=[Ei(-kd)+Ei(kd)]/2$ can also be used (see part B of Appendix). Substituting the three terms in equation (21*a*) and applying condition $y=d$, equation (21*a*) is

$$gka-ka\sigma\left(C-\frac{u_*}{k_v}\ln\frac{d}{k_s}-U_c\right)\mathrm{cth}(kd)+k^2a\left(C-\frac{u_*}{k_v}\ln\frac{d}{k_s}-U_c\right)\left(\frac{u_*}{k_v}\right)\ln\frac{d}{k_s}\cdot\mathrm{cth}(kd)-$$

$$-\frac{k^2a}{\mathrm{sh}(kd)}\left(C-\frac{u_*}{k_v}\ln\frac{d}{k_s}-U_c\right)\left(\frac{u_*}{k_v}\right)T_1+k^2a\bar{U}\left(C-\frac{u_*}{k_v}\ln\frac{d}{k_s}-U_c\right)\mathrm{cth}(kd)=0.$$

Once again, applying shallow water approximation, i.e., $\mathrm{ch}(kd)\approx 1$, $\mathrm{sh}(kd)\approx kd$ and $\mathrm{th}(kd)\approx kd$, the above equation becomes

$$gka(kd)-ka\sigma\left(C-\frac{u_*}{k_v}\ln\frac{d}{k_s}-U_c\right)+k^2a\left(C-\frac{u_*}{k_v}\ln\frac{d}{k_s}-U_c\right)\left(\frac{u_*}{k_v}\right)\ln\frac{d}{k_s}-$$

$$-k^2a\left(C-\frac{u_*}{k_v}\ln\frac{d}{k_s}-U_c\right)\left(\frac{u_*}{k_v}\right)T_1+k^2aU_c\left(C-\frac{u_*}{k_v}\ln\frac{d}{k_s}-U_c\right)=0.$$

Taking round bracket common from second, third and fifth terms, the last equation takes the form

$$gka(kd)+k^2a\left(C-\frac{u_*}{k_v}\ln\frac{d}{k_s}-U_c\right)\left(\frac{u_*}{k_v}\ln\frac{d}{k_s}+U_c-C\right)-$$

$$-k^2a\left(C-\frac{u_*}{k_v}\ln\frac{d}{k_s}-U_c\right)\left(\frac{u_*}{k_v}\right)T_1=0,$$

$$\left(C-\frac{u_*}{k_v}\ln\frac{d}{k_s}-U_c\right)^2+\left(C-\frac{u_*}{k_v}\ln\frac{d}{k_s}-U_c\right)\left(\frac{u_*}{k_v}\right)T_1-gd=0.$$

This quadratic equation provides close form solution for celerity as

$$C=\frac{u_*}{2k_v}\left[\ln\frac{d}{k_s}-\frac{(kd)^2}{4}\right]+U_c\pm\frac{1}{2}\sqrt{\left(\frac{u_*}{k_v}\right)^2\left[\ln\frac{d}{k_s}+\frac{(kd)^2}{4}\right]^2+4gd}\ , \qquad (22)$$

where $T_1=\ln(d/k_s)+(kd)^2/4$ was substituted. The positive sign in expression (22) is for the waves following current (WFC) whereas the negative sign is for the waves opposing current (WOC). The dispersion relation implicit in σ can be found from equation (22) as

$$\sigma = \frac{u_* k}{2k_v}\left[\ln\frac{d}{k_s} - \frac{(kd)^2}{4}\right] + U_c k \pm \frac{1}{2}\sqrt{\left(\frac{u_* k}{k_v}\right)^2\left[\ln\frac{d}{k_s} + \frac{(kd)^2}{4}\right]^2 + 4k^2 gd} \ . \quad (23)$$

Equations (22) and (23) are valid for shallow water waves.

If $u_* = 0$ (i.e., shear is removed from the steady velocity) and $U_c = \overline{U}$ is substituted in equation (23), it reduces to the well established dispersion equation for sine wave over depth-wise constant current $\sigma = k\overline{U} \pm \sqrt{g\,k\,\mathrm{th}(kd)}$ [9]; with shallow wave approximation $\mathrm{th}(kd) \approx kd$, the relationship is

$$\sigma = k\overline{U} \pm k\sqrt{gd} \ . \quad (23a)$$

Moreover, the current component can be eliminated to get wave-only case by substituting $u_* = U_c = 0$ in equation (23). For this substitution, equation (23) reduces to the well-known dispersion equation $\sigma^2 = gk\mathrm{th}(kd)$ and with $\mathrm{th}(kd) \approx kd$, it is

$$\sigma = k\sqrt{gd} \ . \quad (23b)$$

Thus equation (23) includes all the cases and has wide applicability. Similarly, celerity for the above cases also can be obtained from equation (22) by the same substitutions.

To observe the performance of equation (23), some sample values of kd have been computed within shallow wave range ($d/L < 0.05$) for the cases of $d/L = 0.049$, 0.041, 0.035 and 0.031. The corresponding values of $kd = 0.31$, 0.26, 0.22 and 0.2 respectively. The constant-current velocity $\overline{U} = 0.5 \text{ m·s}^{-1}$ is calculated by averaging equation (1) over flow depth and the corresponding shear velocity is an order less than $\overline{U}$, i. e., 0.04 m·s^{-1}. A roughness coefficient $k_s \sim 1$ mm is considered assuming concrete-lined bottom. For the old concrete, k_s will be higher and for the natural bottoms like rivers or coastal areas, $k_s >> 1$ mm.

The wave frequency for these above sample cases is computed from equation (23) and plotted in Fig. 2 for the wave-log current, wave-constant current and wave-only cases. Note that the negative values below x-axis in these figures denote WOC case and therefore their magnitudes (absolute values) should be considered for comparison. Fig. 2 shows that equation (23) is consistent with the well established trend, $\sigma \propto d^{1/2}$ by equations (23a) and (23b), for both WFC and WOC (consider magnitudes of negative values). Fig. 3 if viewed from vertical axis, also facilitate comparison between frequencies. Introduction of concurrent shear reduces σ compare to no-shear (constant current) case. This supports the observation in [2] where is reasoned that this reduction is caused by shear velocity which induces distortion in eddy viscosity at the surface and reduces near bottom friction velocity. Both these effects are minimal in case of WOC and therefore in contrast to WFC, σ in opposing current is higher for the log-current case. Similar trends have noticed in the experiments [24, 39, 40] and in numerical investigation [41]. Moreover, Fig. 2 shows higher σ for with-current cases than σ for no-current case, consistent with the investigation in [9] where is stated that σ should increase in presence of current. Furthermore, the difference between the σ value of log-current and constant-current interaction is amplifying with *kd*. Same amplification can be realized along vertical axis with respect to σ of wave-only case. As $\sigma \propto d^{1/2}$, both the trends suggest increasing influence of shear for higher values of d/L. This confirms greater effect of shear if short period waves are passed on the shear current.

Fig. 2 also shows that, for either of the interactions (wave-log current and wave-constant current), the magnitude of σ is higher for following current than for opposing current for the sample cases described above. However, it is observed in calculations of equation (23) that in wave-constant current interaction, if $\overline{U}$ is decreased, then both the frequencies of WFC and WOC tend to merge to frequency of wave-only case. In wave-log current case, the same observation showed that if shear velocity reduced, then initially higher σ of WFC becomes lower than WOC. In other words, unlike wave-constant current case, reduction in shear velocity reverses the comparative magnitudes of σ between WFC and WOC.

Fig. 2 shows the outcome of equation (23) for the sample cases described above. However, the $k_s > 3$ mm for the old concrete bottom and is much higher for unlined bottom like in natural streams and coastal zones. For these practical situations, high value of k_s results in σ becomes higher in log-current case than constant-current case for WFC. Similarly for WOC, σ reduces in log-current case than constant-current case. These trends are as against of that shown in Fig. 2. This confirms the importance of shear velocity, in turn suggests that shear current should not be approximated by constant-current. Comparison of all the cases described above with percentage change in wave frequency is tabulated in Table 1.

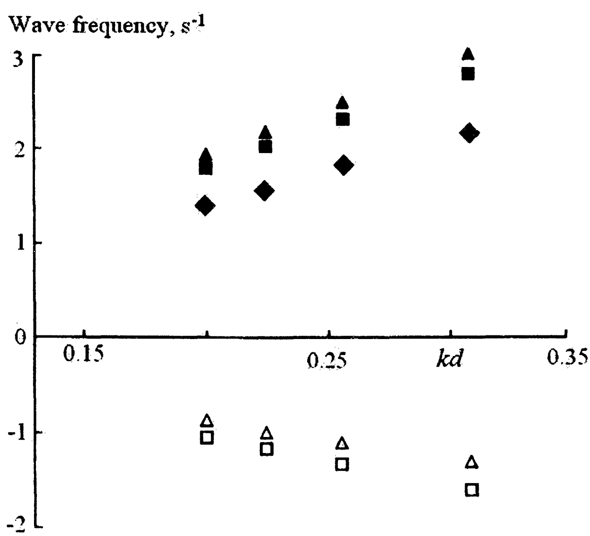

Fig. 2. Change in the wave frequency with *kd* within shallow wave limit. Notations: ▲ – wave-constant current; ■ – wave-log current; ♦ – wave-only case. Dark symbols correspond to the wave following current (WFC), open symbols correspond to the wave opposing current (WOC)

Table 1

The increase in wave frequency (in %) for the cases WFC (wave flowing current) and WOC (wave opposing current)

kd	Increase in σ in WFC over WOC, %		Increase in σ in log-current over constant-current case, %		Increase in σ in log-current over wave-only case, %		Increase in σ in constant-current over wave-only case, %	
	log-current	con-stant-current	WFC	WOC	WFC	WOC	WFC	WOC
0.31	73.30	123.70	−7.34	20.30	28.77	−34.58	38.22	−61.86
0.28	73.39	123.70	−7.32	20.22	28.79	−34.63	38.22	−61.86
0.24	73.44	123.70	−7.31	20.20	28.80	−34.66	38.22	−61.86
0.20	73.48	123.70	−7.30	20.18	28.81	−34.68	38.22	−61.86

5. Second order semi-empirical wave surface and stream function. An attempt is given to derive second order expansion that allows three terms in equations (8) and (9) for η and ψ, respectively as

$$\eta(x,t) = d + a_1 \cos(kx - \sigma t) + a_2 \cos 2(kx - \sigma t) \tag{24}$$

and

$$\psi(x,y,t) = A_o(y) + A_1(y) \cos(kx - \sigma t) + A_2(y) \cos 2(kx - \sigma t), \tag{25}$$

where $a_1 = a$ is the amplitude of wave as described before, a_2 is the coefficient of the second order term and $A_i(y)$, $i = 0$, 1 and 2, are coefficients of equation (25), to be determined.

The same procedure for first order formulation is followed which reveals $A_o = \frac{u_*}{k_v}(y \ln\frac{y}{k_s} - y) + \overline{U}\, y + B_3$ and $A_1(y) = B_4 \,\mathrm{sh}(ky)$, same as first order whereas $A_2(y) = B_5 \,\mathrm{sh}(2ky)$. Thus for $B_3 = 0$, equation (25) can be rewritten as

$$\psi(x,y,t) = \frac{u_*}{k_v}\left(y \ln\frac{y}{k_s} - y \right) + \overline{U} y + B_4 \,\mathrm{sh}(ky)\cos(kx - \sigma t) + B_5 \,\mathrm{sh}2(ky)\cos 2(kx - \sigma t). \tag{26}$$

Further, the second order of the kinematic boundary condition (5) shall provide expressions for B_4 and B_5. Thus second order expansion of equation (5) can be written as

$$\frac{\partial\eta}{\partial t} + \frac{\partial\psi}{\partial y}\frac{\partial\eta}{\partial x} + \frac{\partial\psi}{\partial x} + \eta\frac{\partial\eta}{\partial x}\frac{\partial^2\psi}{\partial y^2} + \eta\frac{\partial^2\psi}{\partial x\partial y} = 0. \tag{27}$$

Substituting equations (24) and (26) in equation (27) and applying $y = d$, the first order terms (i. e. coefficients of $\sin(kx - \sigma t)$) provides equation (19) as a solution for B_4 in equation (26) whereas the collection of coefficients of $\sin 2(kx - \sigma t)$ provides expression for B_5 as

$$B_5 = \frac{a_1^2}{\text{sh}(2kd)}\left[\frac{a_2}{a_1^2}\left(C - \frac{u_*}{k_v}\ln\frac{d}{k_s} - U_c\right) - \frac{u_*}{k_v d}\left(\frac{1}{4} - \frac{a_2 d}{a_1^2}\right) - \frac{k}{4}\left(C - \frac{u_*}{k_v}\ln\frac{d}{k_s} - U_c\right)\text{cth}(kd)\right]. \quad (28)$$

The only unknown in equation (28) is a_2. From the second order expansion of dynamic free surface boundary condition (see, equation (6)), a_2 as a function of a_1 can be found out, however the analysis is difficult for wave-log current flow. As such, B_5 has been obtained empirically using past experimental data. First, a functional relationship for B_5 based on equation (28) is formed as

$$B_5 = f\left\{\frac{a_1^2}{\text{sh}(2kd)},\ C - \frac{u_*}{k_v}\ln\frac{d}{k_s} - U_c\right\}. \quad (29)$$

The two independent variables on the right hand side of equation (29) include all the wave and current parameters. Equation (28) shows nonlinear relationships between B_5 and these independent variables. However, from equation (19), it can be judged that the variable $a_1^2/\text{sh}(2kd)$ would have maintained, had the analytical solution of B_5 been obtained. This fact can be confirmed from the same expression obtained in paper [17] for wave-linear current interaction. As such, B_5 as the nonlinear function of the independent variables is expressed as

$$B_5 = \frac{a_1^2}{\text{sh}(2kd)}\left(C - \frac{u_*}{k_v}\ln\frac{d}{k_s} - U_c\right)^{\phi}, \quad (30)$$

where ϕ is the regression coefficient to be determined from experimental data. The term $(kx - \sigma t)$ in equation (26) suggests that the experimental data should be within a wave period such as wave spectrum. Therefore, a theoretical expression of wave spectrum within a wave period at $y = d$ is derived. Substituting equations (30) and (19) in equation (26), the vertical velocity is derived from equation (26) as

$$W = \frac{\partial \eta}{\partial t} = -\frac{\partial \psi}{\partial x} =$$

$$= ak\left(C - \frac{u_*}{k_v}\ln\frac{d}{k_s} - U_c\right)\sin(kx - \sigma t) + 2ka^2\left(C - \frac{u_*}{k_v}\ln\frac{d}{k_s} - U_c\right)^{\phi}\sin 2(kx - \sigma t). \quad (31)$$

Integrating equation (31) with respect to t, the surface wave spectrum η is derived as

$$\eta = \frac{a}{C}\left(C - \frac{u_*}{k_v}\ln\frac{d}{k_s} - U_c\right)\cos(kx - \sigma t) + \frac{a^2}{C}\left(C - \frac{u_*}{k_v}\ln\frac{d}{k_s} - U_c\right)^{\phi}\cos 2(kx - \sigma t). \quad (32)$$

Experiments of papers [3, 5 – 7] have been noticed, all within intermediate wave range of d/L = 0.1 to 0.2. The data of papers [5 – 7] maintained constant depth and wave period for all waves. However, paper [3] relates to four experimental runs with variable wave period which results in four wave spectrums for different wave periods. Therefore his data (Table 2) used to find ϕ from equation (32) by least square method.

In paper [3] the uniform velocity 0.12 $m \cdot s^{-1}$ corresponds to the no-wave cases whereas the wave data is from four wave-only cases. The author passed these waves over the uniform velocity and measured the change in the wave spectrum due to interaction. This resultant spectrum of wave-current interaction is reproduced in Fig. 3 along with the theoretical wave spectrum by equation (32). A phase shift of $\pi/2$ is provided to the cosine spectrum of equation (32) for in phase matching with the observed data which is in sine spectrum (Fig. 10 in paper [3]). The value of $\phi = 10$ to 16 has been observed (Table 2). Some discrepancies are still observed, the reasons may be because the current

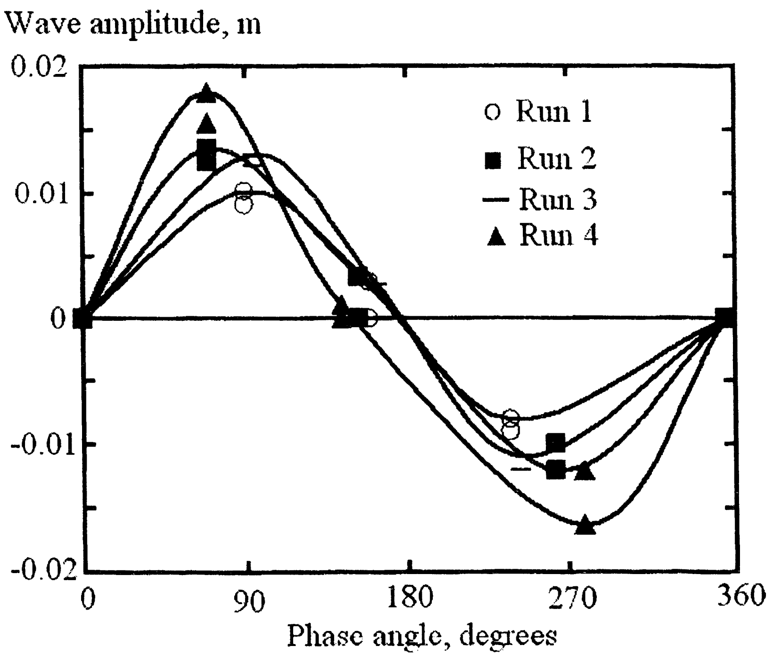

Fig. 3. Surface wave spectrums of wave-log current flows. Notations: lines with symbols – equation (32); symbols only – experimental data from paper [3].

Table 2

The flow and wave data from paper [3]

Experiment	Flow depth, m	Uniform velocity, $m \cdot s^{-1}$	Wave amplitude, m	Wave length, m	Wave period, s	ϕ for combine wave-log-current
Run 1	0.2	0.12	0.0101	1.05	0.9	15
Run 2	0.2	0.12	0.01255	1.21	1.0	16
Run 3	0.2	0.12	0.01335	1.52	1.2	10
Run 4	0.2	0.12	0.014	1.82	1:4	15

in experiments is close to semi-empirical power series that deviates from the usual logarithmic profile (see, equation (1)) used herein. Thus, more experiments on combine flow of sinusoidal wave over log-current are needed for better estimation of ϕ.

Using equation (19) for B_4 and equation (30) for B_5 and proper section of ϕ, the stream function for the combine wave-log current to the second order can be written as

$$\psi(x,y,t) = \frac{u_*}{k_v}\left(y\ln\frac{y}{k_s} - y\right) + U_c y + a\left(C - \frac{u_*}{k_v}\ln\frac{d}{k_s} - U_c\right)\frac{\mathrm{sh}(ky)}{\mathrm{sh}(kd)}\cos(kx - \sigma t) + \tag{33}$$
$$+ a_1^2\left(C - \frac{u_*}{k_v}\ln\frac{d}{k_s} - U_c\right)^{\phi}\frac{\mathrm{sh}(2ky)}{\mathrm{sh}(2kd)}\cos 2(kx - \sigma t),$$

whereas the expression for wave surface to the second order is given by equation (32).

6. Properties of wave-log current flow field (to first order). The properties of the wave-log current flow to the first order are derived based on first order stream function (Eq. 20) and described below. The horizontal and vertical components of the velocity and acceleration are respectively

$$u_x = \frac{u_*}{k_v}\ln\frac{y}{k_s} + U_c + ak\left(C - \frac{u_*}{k_v}\ln\frac{d}{k_s} - U_c\right)\frac{\mathrm{ch}(ky)}{\mathrm{sh}(kd)}\cos(kx - \sigma t), \tag{34}$$

$$u_y = ak\left(C - \frac{u_*}{k_v}\ln\frac{d}{k_s} - U_c\right)\frac{\mathrm{sh}(ky)}{\mathrm{sh}(kd)}\sin(kx - \sigma t) \tag{35}$$

and

$$a_x = a\sigma k\left(C - \frac{u_*}{k_v}\ln\frac{d}{k_s} - U_c\right)\frac{\mathrm{ch}(ky)}{\mathrm{sh}(kd)}\sin(kx - \sigma t), \tag{36}$$

$$a_y = -a\sigma k\left(C - \frac{u_*}{k_v}\ln\frac{d}{k_s} - U_c\right)\frac{\mathrm{sh}(ky)}{\mathrm{sh}(kd)}\cos(kx - \sigma t), \tag{37}$$

where C is given by equation (22). The trajectory of the particle centred at (x, y) at time $t = 0$ is described by the following equations:

$$X = -\frac{ak}{\sigma}\left(C - \frac{u_*}{k_v}\ln\frac{d}{k_s} - U_c\right)\frac{\mathrm{ch}(ky)}{\mathrm{sh}(kd)}\sin(kx - \sigma t), \tag{38}$$

$$Y = \frac{ak}{\sigma}\left(C - \frac{u_*}{k_v}\ln\frac{d}{k_s} - U_c\right)\frac{\mathrm{sh}(ky)}{\mathrm{sh}(kd)}\cos(kx - \sigma t). \tag{39}$$

The vertical pressure distribution is

$$p=-\rho g(y-d)+\rho a\sigma\left(C-\frac{u_*}{k_v}\ln\frac{d}{k_s}-U_c\right)\frac{\mathrm{ch}(ky)}{\mathrm{sh}(kd)}\cos(kx-\sigma t)-$$
$$-\rho a^2k^2\left(C-\frac{u_*}{k_v}\ln\frac{d}{k_s}-U_c\right)^2\frac{1-\mathrm{ch}(2ky)}{4\,\mathrm{sh}^2(kd)}. \quad (40)$$

The mass, momentum and energy fluxes [42] in the rotational flow field to the first order approximation are given respectively as

$$Q=\rho d\frac{u_*}{k_v}\ln\frac{y}{k_s}+\rho U_c d+a\left(C-\frac{u_*}{k_v}\ln\frac{d}{k_s}-U_c\right)\frac{\mathrm{sh}(ky)}{\mathrm{sh}(kd)}\cos(kx-\sigma t)+O(a^2k^2), \quad (41)$$

$$M=\frac{\rho g d^2}{2}+\frac{\rho\sigma a}{k}\left(C-\frac{u_*}{k_v}\ln\frac{d}{k_s}-U_c\right)\cos(kx-\sigma t)+O(a^2k^2), \quad (42)$$

$$E=-\rho g\frac{u_*d^2}{2k_v}\left(\frac{3}{2}-\ln\frac{y}{k_s}\right)-a\rho g\left(C-\frac{u_*}{k_v}\ln\frac{d}{k_s}-U_c\right)\frac{1-\mathrm{ch}(ky)}{k\,\mathrm{sh}(kd)}\cos(kx-\sigma t)+$$
$$+\frac{a\rho\sigma u_*}{k_v k\,\mathrm{sh}(kd)}\left(C-\frac{u_*}{k_v}\ln\frac{d}{k_s}-U_c\right)\left[\ln\frac{y}{k_s}\mathrm{sh}(kd)-\ln\frac{d}{k_s}-\frac{(kd)^2}{4}\right]\cos(kx-\sigma t)+ \quad (43)$$
$$+\frac{a\rho\sigma}{k}U_c(C-U_c)\cos(kx-\sigma t)+\frac{1}{2}\rho g d U_c(d-y)+O(a^2k^2).$$

The irrotational flow properties for the wave-constant current in shallow waves can be obtained by substituting $u_*=0$ in the above expressions. The corresponding celerity, i.e., $C=\overline{U}+\sqrt{gd}$, may be obtained by substituting $u_*=0$ and $U_c=\overline{U}$ in equation (22). Further substitution of $u_*=U_c=0$; provides properties for wave-only case and for which equation (22) becomes $C=\sqrt{gd}$.

7. Discussion and conclusions. This study presents the change in the permanence and properties of regular shallow waves in the presence of vertically logarithmic current and can serve as a ground work for possible applications and advances. The resultant stream function and wave surface describes the nonlinear interaction of the combine wave-log current flow field. A close form solution of the corresponding dispersion equation (equation (23)) is derived for shallow wave approximation and is different in structure than that derived by [17] for wave-linear current. Equation (23) reveals several features of WFC and WOC in three types of flow fields, wave-log current, wave constant-current and wave-only cases. Table 1 presents the estimate of frequencies for these flows for $kd<0.314$, i.e. within shallow wave range. Presence of logarithmic shear in following direction enhances pure wave frequency by 29% whereas it is 38% in presence of constant current. These increased values over wave-only case are due to the dominant distortion in eddy viscosity at surface in presence of a following current. Some contrary mechanisms like wave damping and curvature of eddy viscosity over flow depth tends to reduce σ but are cancelled out by additional supportive mechanisms like wave-induced Reynolds' stress reduced friction velocity in bottom boundary layer [2]. The difference of 9% can be attributed to the distortion effect in presence of constant-current. This difference matches with the calculated value of 7% (Table 1, 4th column) for the wave following current if constant current is replace by logarithmic shear.

The trend described above reverses in opposing current. The reduction in σ over wave-only case is just 35% in presence of logarithmic shear whereas it is 62% is constant-current is assumed. This suggests rather strong effect of contrary mechanisms than supportive ones. The difference of 27% matches with the calculated value of 20% (Table 1, 5th column) for the WOC if constant current is replaced by logarithmic shear. Furthermore, change in flow direction causes 73% change in σ in case of log-current whereas it is 124% in case of constant current. This confirms stronger influence of surface distortion of eddy viscosity in presence of constant current than log-current. Physically, the above statistics concludes that wave speed increases in WFC but the increase in wave speed is slower in log-current than constant-current. In case of WOC, the wave speed reduces and the reduction is slower in log-current than constant-current case. Moreover for high roughness like natural beds, the magnitude of d/k_s shall reduce, reflecting shallower water depth and for a given wavelength, wave frequency of log-current will be higher than that of constant-current for WFC and vice versa for WOC. This can be judged from Fig. 2 in which the left side extrapolation of constant-current and log-current data is crossing each other in both the WFC and WOC cases. These observations show the difference in wave-current properties in presence of shear effect, in turn recommends that presence of shear current should not be approximated by constant current.

The present model of dispersion equation follows all the established trends for wave-constant current flow fields. The method of combine formulation used for wave-log current (i) removes the possible errors involved when depth-wise log-current is approximated by depth-wise constant or linear current, (ii) removes the biases which exist when both the hydrodynamics (wave and log-current) are not considered concurrently. The formulation also provides expressions for the cases of wave-constant current flow and wave-only flow, by simply substituting $u_* = 0$ or $u_* = 0$ and $\overline{U} = 0$, respectively.

The wave-log current model presented herein can be useful in accurate prediction of dispersion of physico-chemical transport in uniform flow with wind waves, impacts on marine life being important in the coastal zone and in flow studies on vegetation where small change in the horizontal log-velocity result in twice as large change in drag force. The application of such model can be extensive, in modeling the physical hydrology, morphological evolution, sedimentology and toxicology of a wide range of shallow water settings. Some of the finer studies like amount of wave damping, surface distortion of eddy viscosity change in the turbulent stresses and bottom friction velocity can be studied when the shear flow is vertically logarithmic. The present formulation can also be a guideline for hydrodynamic laboratories where waves are to be generated over the steady log-current to conduct testing and simulation studies.

Appendix

A. Solution via exponential series. The integration of $\Im$ by parts leads to

$$\Im = \int \ln\frac{y}{k_s}\,\mathrm{sh}(ky)dy = \frac{1}{k}\ln\frac{y}{k_s}\mathrm{ch}(ky) - \frac{1}{k}\int\frac{1}{y}\mathrm{ch}(ky)dy.$$

It can be noted that derivative of log term can be written as $\frac{d}{dy}\left(\ln\frac{y}{k_s}\right) = \frac{1}{y}$.
When this result is integrated, it will be $\int(1/y)dy = \ln y + C_i$, where C_i is the constant of integration and its value should be $C_i = -\ln k_s$ to get back the original logarithmic function. Thus the solution of $\int(1/y)dy = \ln(y/k_s)$. The following derivation follows these solutions

$$\int\frac{1}{y}\mathrm{ch}(ky)dy = \frac{1}{2}\left(\int\frac{e^{ky}}{y}dy + \int\frac{e^{-ky}}{y}dy\right). \tag{A1}$$

The integrals in formula (A1) can be written in the form of a series as

$$\int\frac{e^{\pm ky}}{y}dy = \ln\frac{y}{k_s} \mp \frac{ky}{1!} + \frac{k^2y^2}{2\cdot 2!} \mp \frac{k^3y^3}{3\cdot 3!} + \ldots. \tag{A2}$$

Substituting expressions (A2) in relation (A1), the odd terms cancel. Thus integral (A1) is

$$\int\frac{1}{y}\mathrm{ch}(ky)dy = \ln\frac{y}{k_s} + \sum_{n=1}^{\infty}\frac{(ky)^{2n}}{2n\cdot 2n!}. \tag{A3}$$

For the waves in shallow water, $d/L < 0.05$, $kd = 2\pi d/L < 0.314$. As such, series in equation (A3) can be truncated for $O(kd)^4$ and relation (A3) is simplified as

$$\int\frac{1}{y}\mathrm{ch}(ky)dy \approx \ln\frac{y}{k_s} + \frac{(ky)^2}{4}. \tag{A4}$$

Thus, a close form solution for the shallow wave approximation can be obtained as

$$\Im = \int\ln\frac{y}{k_s}\mathrm{sh}(ky)dy \approx \frac{1}{k}\ln\frac{y}{k_s}\mathrm{ch}(ky) - \frac{1}{k}\left[\ln\frac{y}{k_s} + \frac{(ky)^2}{4}\right]. \tag{A5}$$

Applying the condition $y = d$ to be satisfied at mean surface, the solution is

$$\Im \approx \frac{1}{k}\ln\frac{d}{k_s}\mathrm{ch}(kd) - \frac{1}{k}\left[\ln\frac{d}{k_s} + \frac{(kd)^2}{4}\right].$$

B. Solution via Ei(z) function (exponential integral function). The integration of $\Im$ by parts leads to

$$\Im = \int \ln\frac{y}{k_s}\,\mathrm{sh}\,(ky)dy = \frac{1}{k}\ln\frac{y}{k_s}\,\mathrm{ch}(ky) - \frac{1}{k}\int\frac{1}{y}\mathrm{ch}(ky)dy$$

in which

$$\frac{1}{k}\int\frac{1}{y}\mathrm{ch}(ky)dy = \frac{1}{2k}\int\left(\frac{e^{x_1}}{x_1}+\frac{e^{-x_1}}{x_1}\right)dx_1 = \frac{1}{2k}\left[\mathrm{Ei}(-ky)+\mathrm{Ei}(ky)\right],$$

where $x_1 = ky$. Thus,

$$\Im = \int \ln\frac{y}{k_s}\,\mathrm{sh}\,(ky)dy = \frac{1}{k}\ln\frac{y}{k_s}\,\mathrm{ch}(ky) - \frac{1}{2k}\left[\mathrm{Ei}(-ky)+\mathrm{Ei}(ky)\right]. \qquad \text{(B1)}$$

Applying the condition $y = d$ to be satisfied at mean surface, the formula (B1) is

$$\Im = \frac{1}{k}\ln\frac{d}{k_s}\cdot\mathrm{ch}(kd) - \frac{1}{2k}\left[\mathrm{Ei}(-kd)+\mathrm{Ei}(kd)\right].$$

The values of Ei(z) can be found from standard mathematical tables [43]. In general the solution can be written as

$$\Im = \frac{1}{k}\ln\frac{d}{k_s}\cdot\mathrm{ch}(kd) - T_1, \qquad \text{(B2)}$$

where $T_1 = \frac{1}{2k}\left[\mathrm{Ei}(-kd)+\mathrm{Ei}(kd)\right]$ or $T_1 = \frac{1}{k}\left[\ln\frac{d}{k_s}+\frac{(kd)^2}{4}\right]$.

References

1. *Whitham G.B.* Linear and Nonlinear Waves. –Wiley, New York, 1974. – 636 pp.
2. *Huang Z., Mei C.C.* Effects of surface waves on turbulent current // J. Fluid Mech. – 2003. – 497. – P. 253 – 287.
3. *Umeyama M.* Reynolds stresses and velocity distributions in a wave-current coexisting environment // J. Waterway, Port, Coastal, and Ocean Engineering. – 2005. – 131, No 5. – P. 203 – 212.
4. *Mei C.C., Jin K.R., Fan S.J.* Resuspension and transport of fine sediments by 412 waves // J. Geophys. Res. – 1997. – 102, No C7. – P. 15807 – 15821.
5. *Kemp P.H., Simons R.R.* The interaction between waves and a turbulent current: waves propagating with the current // J. Fluid Mech. – 1982. – 116. – P. 227 – 250.
6. *Kemp P.H., Simons R.R.* The interaction between waves and a turbulent current: waves propagating against the current // J. Fluid Mech. – 1983. – 130. – P. 73 – 89.
7. *Klopman G.* Vertical structure of the flow due to waves and currents // Delft Hydraulics. – Progress Report, No. H840.30, Part II, prepared for Rijkwaterstaat, Tidal WaterDivision and Commission of the European Communities, Directorate General XII, Delft, The Netherlands. – 1994.
8. *Airy G. B.* Tides and waves. – Encyclopedia Metropolitana. – 1845. – 5. – P. 241 – 396.

9. *Dean R.G., Dalrymple R.A.* Water Wave Mechanics for Engineers and Scientists. – Prentice Hall, World Scientific, Singapore, 1991. – 353 pp.
10. *Chappelear J.E.* Direct numerical calculation of wave properties // J. Geophys. Res. – 1961. – 66, No 2. – P. 501 – 508.
11. *Dean R.G.* Stream function representation of nonlinear ocean waves // J. Geophys. Res. – 1965. – 70, No 18. – P. 4561 – 4572.
12. *Teng B., Zhao M., Bai W.* Wave diffraction in a current over a local shoal // Coastal Engineering. – 2001. – 42, No 22. – P. 163 – 172.
13. *Tsao, S.* Behaviour of surface waves on a linearly varying current // J. Geophys. Res. – 1957. – 79, – P. 4498 – 4508.
14. *Dalrymple R.A.* A finite amplitude wave on a linear shear current // J. Geophys. Res. – 1974. – 79, No 30. – P. 4498 – 4504.
15. *Simmen J.A., Saffman P.G.* Steady deep-water waves on a linear shear current // Studies in Applied Mathematics. – 1985. – 73, – P. 35 – 57.
16. *Dalrymple R.A.* A numerical model for periodic finite amplitude wave on a rotational fluid // J. Comput. Phys. – 1977. – 24, No 1. – P. 29 – 42.
17. *Baddour R.E., Song S.W.* The rotational flow of finite amplitude periodic water waves on shear current // Applied Ocean Res. – 1998. – 20, No 3. – P. 163 – 171.
18. *Longuet–Higgins M.S., Stewart R.W.* The changes in amplitude of short gravity waves on steady non-uniform currents // J. Fluid Mech. – 1961. – 10, No 4. – P. 529 – 549.
19. *Thompson P.D.* The propagation of small surface disturbance through rotational flow // Ann. N. Y. Acad. Sci. – 1949. – 51, No 3. – P. 463 – 474.
20. *Taylor G.I.* The action of a surface current used as a breakwater // Proc. Roy. Soc. London, A. – 1955. – A231. – P. 466 – 478.
21. *Brevik I.* The stopping of linear gravity waves in current of uniform vorticity // Physica Norvegica. – 1976. – 8, No 1. – P. 157 – 162.
22. *Dalrymple R.A.* A Finite Amplitude Wave on Linear Shear Current // J. Geophys. Res. – 1974. – 79, No 30. – P. 4498 – 4504.
23. *Dalrymple R.A.* Water wave models and wave forces with shear currents // Coastal Ocean Eng. Lab. – Tech. Report. – 1973. – No 20. – Univ. of Florida, Gainesville. – 163 pp.
24. *Bakker W.T., Van Doorn T.* Near-bottom velocities in waves with a current // Proc. 16th Conf. on Coastal Eng. – Hamburg, Germany, 1978. – P. 1394 – 1413.
25. *Russell J.M.* A survey of exact solutions of inviscid field equations in the theory of shear flow instability // Appl. Sci. Res. – 1994. – 53, No 1 – 2. – P. 163 – 186.
26. *Umeyama M., Gerritsen F.* Velocity distribution in uniform sediment-laden flow // J. Hydraul. Eng. – 1992. – 118, No 2. – P. 229 – 245.
27. *Peregrine D.H.* Interaction of water waves and currents // Adv. Appl. Mech. – 1976. – 16.– P. 9 – 117.
28. *Margaretha H.* Mathematical modelling of wave-current interaction in a hydrodynamic laboratory basin. – PhD Thesis, 2005. – University of Twente, Netherlands. – 116 pp.
29. *Abdullah A.J.* Wave motion at the surface of current which has an exponential distribution of vorticity // Ann. N. Y. Acad. Sci. – 1949. – 51, No 3. – P. 425 – 441.
30. *Wehausen J.V.* Free surface flows. Research frontiers in fluid dynamics // R. J. Seeger and G. Temple Eds., Inter-science. – 1965. – P. 534 – 640.
31. *Eliasson J., Engelund F.* Gravity waves in rotational flow // Inst. of Hydrodynamics and Hydr. Eng. Tech., Univ. of Denmark, Lyngby. – Prog. Report No 26. – 1972. – P. 15 – 22.
32. *Dalrymple R.A., Cox J.C.* Symmetric finite amplitude rotational water waves // J. Phys. Oceanogr. – 1976. – 6, No 6. – P. 847 – 852.
33. *Yih C.S.* Surface waves in flowing water // J. Fluid Mech. – 1972. – 51, No 2. – P. 209 – 220.
34. *Fenton J.D.* Some results for surface gravity waves on shear flows // J. Inst. Math. Appl. – 1973. – 12. – P. 1 – 20.
35. *Nepf H.M. and Monismith, S.G.* Wave dispersion on a shear current // Applied Ocean Research. – 1994. – 16, No 5. – P. 313 – 315.
36. *Schlichting H.* Boundary Layer Theory. – 1st Edition. – McGraw-Hill Book Co., New York, 1955. – 647 pp.

37. *Nezu I., Nakagawa H.* Turbulence in open-channel flows. – Balkema Publishers, Rotterdam, Netherlands, 1993. – 281 pp.
38. *Coles D.* The law of the wake in the turbulent boundary layer // J. Fluid Mech. – 1956. – 1, pt. 2. – P. 191 – 226.
39. *Mathisen P.P., Madsen O.S.* Waves and currents over a fixed rippled bed: bottom roughness experienced by waves in the presence and absence of currents // J. Geophys. Res. – 1996. – 101, No C7. – P. 16533 – 16542.
40. *Mathisen P.P., Madsen O.S.* Waves and currents over a fixed rippled bed: bottom roughness experienced by currents in the presence waves // J. Geophys. Res. – 1996. – 101, No C7. – P. 16543 – 16550.
41. *Groeneweg J., Klopman G.* Changes of the mean velocity profiles in the combined wave-current motion in a GLM formulation // J. Fluid Mech. – 1998. – 370. – P. 271 – 296.
42. *Boccotti P.* Wave mechanics for ocean engineering. – Elsevier oceanographic series, NY, 2000. – 496 pp.
43. *Beyer W.H.* CRC standard mathematical tables. – 25th Edition. – CRC Press Inc., Boca Raton, Florida, 2000. – 812 pp.

Biological and Agricultural Engineering,
Texas A & M University, College Station,
Texas, USA

Manuscript received
December 19, 2006